Chapter 2

Chemical Passivation of Ge(111) Surfaces

2.1 Background

A stable, low defect-density GeO_x/Ge interface that is analogous to the SiO_x/Si(100) interface cannot be formed, so the elimination of surface oxide from Ge would be important to the utilization of Ge as a device material. The original surface passivation through Grignard alkylation of a diamond-type semiconductor had in fact been performed on Ge in 1962.[1] The researchers were successful in eliminating the influence of atmospheric moisture upon the electronic properties of the crystal surface, but still suffered from a large density of surface states, possibly because of an overly aggressive etching procedure. Very little follow-up work on such organic passivation methods was done in the ensuing decades. More recent work has shown that a variation on that early procedure is useful in passivating Si surfaces.[2,3] The alkylated Ge(111) surfaces described in this research were prepared in a similar manner, with some modifications. This chapter is a description of the chemical methods utilized.

Proper cleaning of the substrate is crucial to any successful surface modification.

The well established methods for cleaning Si cannot be directly applied to Ge because the oxide offers no protection. Aqueous acidic oxidizing solutions can easily etch and roughen the surface.[4,5] Repeated etching cycles in aqueous acid etchants and water can remove contaminants such as metal ions, but do still remove crystal material and thus leave open the possibility for further surface roughening.[6–10] Degreasing with organic solvents does not etch the surfaces, but does not remove ionic contaminants, so aqueous etching methods cannot be avoided.

Hydrogen-terminated surfaces may be prepared through the use of aqueous HF solutions. Removal of the oxide is possible, but the well-ordered 1x1 H-Si(111) surface established for Si(111) treated with aqueous NH_4F solution has no reported Ge(111) corollary.[11] Confirmation that the NH_4F solutions do not lead to a flat, hydrogen-terminated surface is easily achieved by noting that the etchant does not produce a hydrophobic Ge surface. There is some disagreement over the stability of the H-Ge(111) surface, but it is generally accepted that it does not posses the stability of the H-Si(111) surface.[8,12,13]

Halogen termination can be achieved in vacuum or in solution.[14,15] The distance between Ge atop atoms is approximately 4 Å, which can accommodate bromine or chlorine on every site.[16,17] While not air-stable over long periods, these surfaces do serve as useful precursor substrates for Grignard alkylation.[1,18]

Sulfide passivation of Ge(100) and Ge(111) in UHV conditions had been reported to successfully remove oxygen through the formation of either 1.0 ML or 0.5 ML sulfur atoms bonded to the surface, depending upon the sulfur source and annealing procedure.[19] Such passivation was then attempted with a more readily accessible

wet chemical method involving $(NH_4)_2S$, but an amorphous GeS_x layer was often formed.[12,20,21] Dielectric stacks formed on sulfur-passivated Ge(100) with HfO_2 displayed trap state densities very similar in magnitude to unpassivated stacks.[22] From these results, it appears the sulfide layer formation does not reliably passivate the Ge surface.

Organic passivation can be achieved at relatively low temperatures and could allow further functionalization of the surface. Three methods of attaching long-chain hydrocarbons have been established and are summarized in Figure 2.1. From the hydrogen- or halogen-terminated surface, organic molecules can be attached either through reaction with thiols or with terminal olefins.[12,23–26] The thiol attachment route has the advantage of requiring neither heat nor inert atmosphere, however it has the disadvantage of producing a less chemically robust surface.[23] Hydrogermylation requires only one post-etching step, is completed within a couple of hours, and produces the more chemically inert Ge-C bond at the surface.[25] The Grignard alkylation also produces Ge-C bonds, and is unique in that it allows the attachment of methyl groups to the surface, allowing for the thinnest overlayer and best possible coverage. Larger organic groups, such as ethyl, have a radius of 4.5–5.0 Å, which does not allow for the capping of every atop atom of the Ge(111) surface.[1,27,28]

Because they show the greatest stability and do not require energy-intensive high vacuum techniques, the organic modifications show promise as useful interface passivation methods. This chapter details the experimental procedures for the surface modifications used in the investigations described in the subsequent chapters.

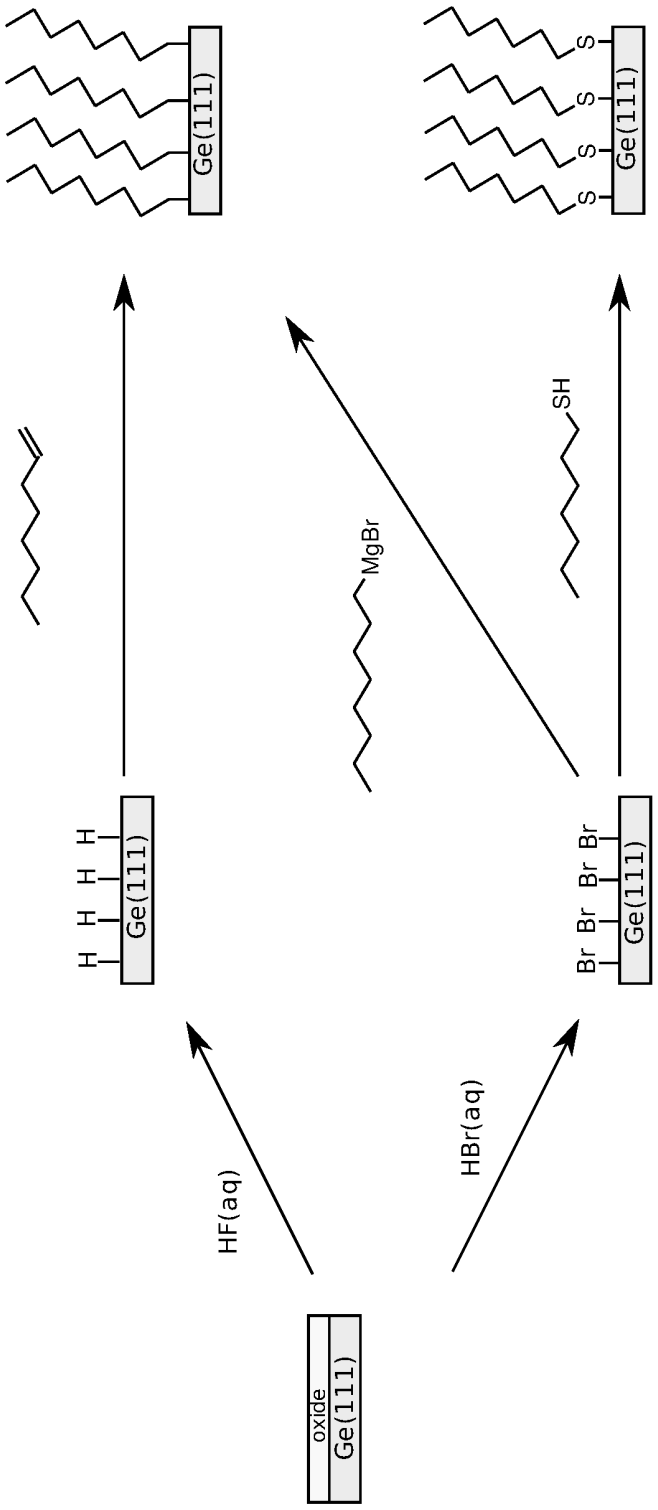

Figure 2.1: Schemes for grafting alkyl monolayers to Ge(111)

2.1.1 X-Ray Photoelectron Spectroscopy

2.1.1.1 Elemental Analysis

X-ray photoelectron spectroscopy (XPS) is useful for surface sensitive elemental analysis and for obtaining certain chemical information such as oxidation state. The sample under ultra-high vacuum is irradiated with a monochromatic X-ray line of sufficient energy to eject core electrons to vacuum, where they are collected by the analyzer and sorted by kinetic energy. The kinetic energy, KE, is a function of the photo-ionized atom, but also the X-ray energy, $h\upsilon$ and the work function, Φ of the specific instrument being used. As a result, the data is usually reported in binding energy, BE

$$BE = h\upsilon - KE - \Phi \tag{2.1}$$

which is independent of the X-ray source and instrument.

Figure 2.2 is a survey spectrum of sputter-cleaned Ge. Many of the features visible in the spectrum are either Auger lines or XPS lines compounded with another energy loss pathway. Random scattering of photoelectrons causes the baseline to rise after every strong emission line. A photo-ionized atom may be in an excited state, or a quantized amount of energy may go into bulk plasmons rather than KE so there are often peaks of less intensity located at higher B. eV from the parent XPS line.

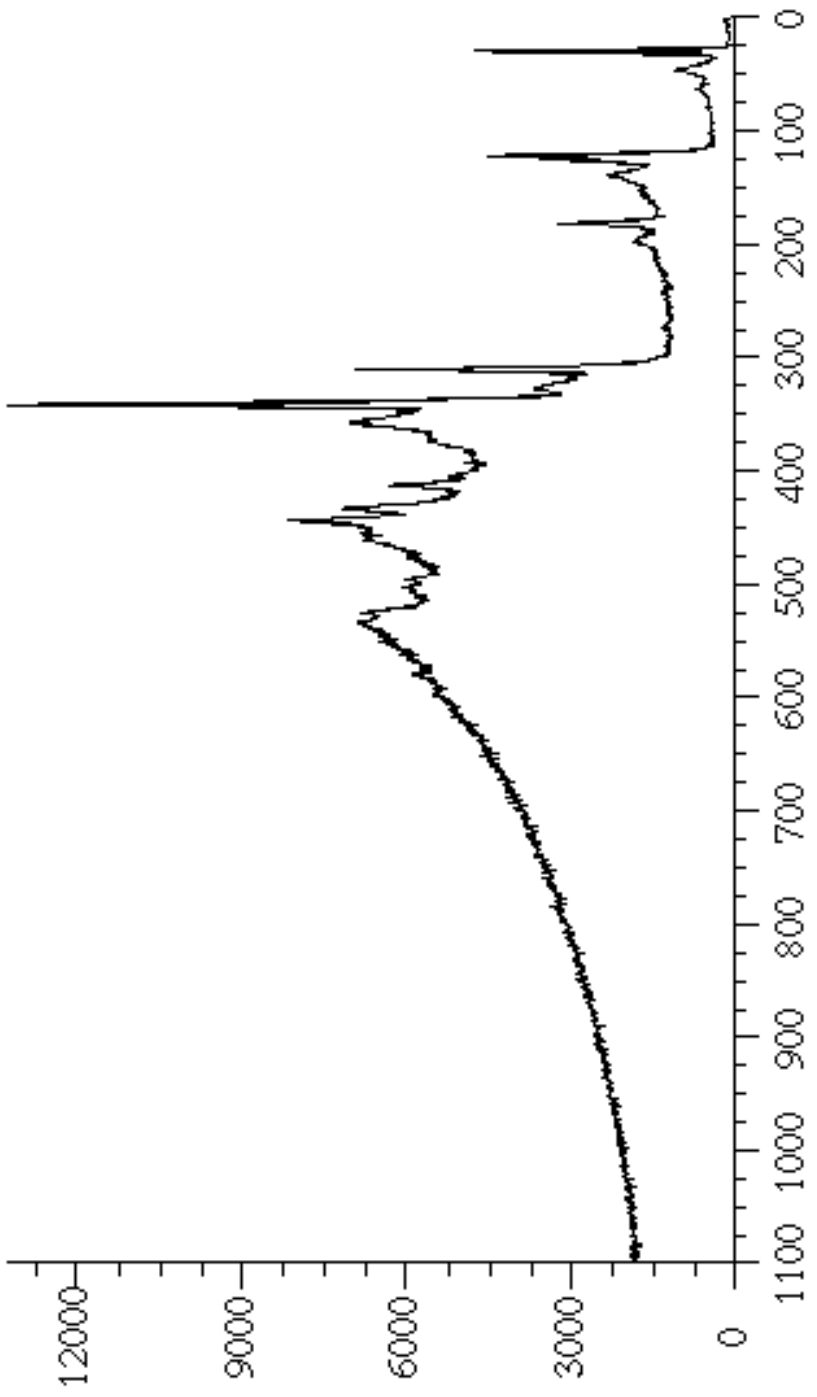

Figure 2.2: XPS survey spectrum of clean Ge

2.1.1.2 Surface Coverage Model

A substrate-overlayer model was used to quantify the composition of the surface region.[29,30] In the following analysis, the X-ray penetration depth far exceeds the photoelectron escape length, λ, so only the escape length affects the XPS line intensity. The escape length is dependent upon the kinetic energy of the photoelectron and the material of the overlayer through which it must travel. This dependence was calculated by the empirical relationship

$$\lambda = 532^{-2} + 0.41a^{1.5}KE^{0.5} \tag{2.2}$$

where a is the atomic diameter.

The spectral peaks of interest in this study are Br $3d$ or C $1s$ of the overlayer atoms and the Ge $3d$ of the crystal surface atoms. Because there will always be hydrocarbon contamination of a surface exposed to air or backstreamed mechanical pump oil, the C $1s$ peak contains a 285 B. eV component arising from carbon bonded to carbon (C-C). A core electron of carbon bonded to a less electronegative element such as Ge (C-Ge) will have a lower binding energy, so for alkylated samples, there is a C $1s$ component at 284.3 B. eV. The area of that component is a measure of the alkyl groups bonded to the surface.

The Ge $3d$ spectral peak is dominated by emission from the crystal atoms below the surface, which yields a doublet at 29.4 and 30 B. eV. The doublet arises from spin orbit coupling, and has a well established peak intensity ratio. Surface Ge atoms are not readily apparent, but those atoms which are in $+1 - +4$ oxidation states, such as

those in an oxide, have a sufficiently higher binding energy to be visible in the 31 – 33 B. eV range, distinguishable from the bulk emission. The intensity of this broad spectral feature is a measure of the chemical oxidation of the Ge surface, as described below.

The thickness of the carbon overlayer is calculated from the C 1s and Ge 3d peak area from

$$\frac{I_{ov}}{I_{Ge}} = \left(\frac{SF_{ov}}{SF_{Ge}}\right)\left(\frac{\rho_{ov}}{\rho_{Ge}}\right)\left[\frac{1-\exp\left(-\frac{d_{ov}}{\lambda_{ov}\sin\theta}\right)}{\exp\left(-\frac{d_{ov}}{\lambda_{Ge}\sin\theta}\right)}\right] \tag{2.3}$$

where is I the peak intensity, ρ is the atomic density, SF is the sensitivity factor, d_{ov} is the overlayer thickness, λ is the photoelectron escape length, and θ is the photoelectron take-off angle determined by the surface orientation relative to the analyzer. The subscript ov signifies an overlayer component, the subscript Ge signifies a Ge component. The Ge 3d spectral peak was chosen over the more surface-sensitive Ge 2p because the 3d photoelectron has a high kinetic energy that is similar to that of the C1s photoelectron, so that $\lambda_{Ge} \approx \lambda_{ov}$ and equation 2.3 may be simplified to

$$d_{ov} = \lambda_{ov}\sin\theta \times \ln\left(1+\left(\frac{SF_{Ge}}{SF_{ov}}\right)\left(\frac{I_{ov}}{I_{Ge}}\right)\left(\frac{\rho_{Ge}}{\rho_{ov}}\right)\right) \tag{2.4}$$

An alternative formulation that is useful for expressing the fractional monolayer coverage from the 284.3 B. eV C 1s component is

$$\left(\frac{I_{ov}}{I_{Ge}}\right) = \frac{\Phi_{ov}\left(1-\exp\left(\frac{-a_{ov}}{\lambda_{ov}\sin\theta}\right)\right)}{1-\Phi_{ov}\left(1-\exp\left(\frac{-a_{ov}}{\lambda_{Ge}\sin\theta}\right)\right)}\left(\frac{\rho_{ov}}{\rho_{Ge}}\right)\left(\frac{SF_{ov}}{SF_{Ge}}\right) \tag{2.5}$$

where Φ_{ov} is the fractional monolayer coverage, and a_{ov} is the atomic diameter of the overlayer. If Φ_{ov} is not large, and the escape lengths are once again set equal, equation 2.5 can be simplified to

$$\Phi_{ov} = \left[\frac{\lambda_{ov}\sin\theta}{a_{ov}}\right]\left(\frac{\rho_{Ge}}{\rho_{ov}}\right)\left(\frac{SF_{Ge}}{SF_{ov}}\right)\left(\frac{I_{ov}}{I_{Ge}}\right) \tag{2.6}$$

Oxygen incorporation was never intentional for these experiments, so the signal from the 532 B. eV O 1s peak was usually weak and difficult to quantify. The GeO_x layer was instead quantified from the Ge 3d peak. From the intensity ratio of the higher B. eV component to the bulk Ge component, the oxide thickness may be calculated in a manner very similar to that used in equation 2.4.

$$d = \lambda_{ov}\sin\theta \times \left(\ln\left[1 + \left(\frac{I^0_{Ge}}{I^0_{ov}}\right)\left(\frac{I_{ov}}{I_{Ge}}\right)\right]\right) \tag{2.7}$$

where the subscript ov denotes the oxide overlayer. The ratio I^0_{Ge}/I^0_{ov} is an experimentally determined normalization factor obtained from the ratio of pure Ge to pure oxide.[29]

To estimate the fraction of surface atoms that are oxidized, the measured Ge 3d ratio is compared to the expected value for 100% oxidation. Because the kinetic energy of all considered photoelectrons are similar, any scattering and attenuation should be similar and may be ignored. The total intensity, used in the relation of equation 2.8, would have contribution from all photoelectrons able to reach the surface, which would depend upon the atomic density (n_{Ge}), the photoionization cross section (σ_{Ge}), and the take-off angle-dependent escape depth (λ_{Ge}).

$$I_{Ge} \approx n_{Ge}\sigma_{Ge}\int_0^\infty \exp\left(-\frac{z}{\lambda_{Ge,bulk}\sin\theta}\right)\mathrm{d}z = n_{Ge}\sigma_{Ge}\lambda_{Ge,bulk}\sin\theta \tag{2.8}$$

The surface atoms have the same photoionization cross section, a two-dimensional surface density ($n_{Ge,s}$), but the photoelectrons do not traverse the bulk material, so the surface contribution can be given by

$$I_{Ge,s} \approx n_{Ge,s}\sigma_{Ge} \tag{2.9}$$

If every surface atom is oxidized, the broad oxidized spectral peak would be given by equation 2.9, and the bulk peak component would be $I_{Ge} - I_{Ge,s}$, so a ratio of 0.223 would be obtained from

$$\frac{I_{Ge,s}}{I_{Ge}} = \frac{n_{Ge,s}}{n_{Ge}\lambda_{Ge,bulk}\sin\theta - n_{Ge,s}} \tag{2.10}$$

and division of the measured ratio by equation 2.10 yields the fraction of oxidized surface atoms.

2.2 Experimental

2.2.1 Materials

Unless stated otherwise, all chemicals were purchased from Aldrich or Alfa Aesar and used as received. All water was obtained from a Barnstead Nanopure system and had a resistivity of 18 MΩ-cm. Diethylene glycol dibutyl ether (DEGDBE) was

vacuum distilled from $LiAlH_4$ and stored under nitrogen until further use. 1-Decene was vacuum distilled from sodium metal and stored under nitrogen, in the dark, until needed. Br_2(l) was vacuum transferred from phosphorus(V) oxide, subjected to multiple freeze-pump-thaw cycles, and stored in a Schlenk flask until needed. Etching solutions were prepared from dilution (or combination) of 30.7 M (49%) HF, 9.7 M (30%) H_2O_2, 12.0 M (37%) HCl, or 8.8 M (48%) HBr.

Dimethylmagnesium solutions were prepared by adding small portions of 1,4-dioxane to methylmagnesium bromide in diethyl ether until the dioxane•$MgBr_2$ complex no longer precipitated, then the ether solution was filtered through glass wool. Low vapor-pressure organomagnesium and organolithim solutions were prepared from the diethyl ether solutions by addition of an equal volume DEGDBE, then vacuum removal of the diethyl ether to a liquid nitrogen cooled trap.

Two-inch Ge(111) wafers (MTI Corp.) were diced with a diamond scribe to form rectangular fragments of a size appropriate for the experiment, and the edges were ground with carbide paper to prevent shattering. When necessary, regions of the surface were sanded for ohmic contact points. The fragments were then rinsed with water and and either degreased with refluxing isopropanol in an extractor apparatus shown in Figure 2.3 on page 24, or sonicated in a detergent solution (7x cleaning solution, MP BioMedical). To remove any contamination in the oxide layer, the fragments were then rinsed with water, immersed in a 30% hydrogen peroxide for 50 – 70 s, then rinsed again and blown dry with nitrogen.

2.2.2 Surface Modification

2.2.2.1 Grignard Alkylation

Each sample was etched until the etchant solution did not adhere to the surface. The etchant compositions and etching durations are listed in Table 2.1. H-Ge(111) surfaces were prepared by one of two methods. Some samples were very briefly etched with an anisotropic etchant, henceforth referred to as Superoxol etch, composed of a mixture of H_2O, HF, and H_2O_2 in a 4:1:1 volume ratio of their standard concentrations to yield a solution of 1.6 M H_2O_2 and 5.1 M HF(aq). These samples were then thoroughly rinsed and placed in a 6.0–9.0 M HF(aq) solution for 3–6 min, until the surface was cleanly hydrophobic. Samples that were not treated with the Superoxol etch were also etched with 6.0–9.0 M HF(aq), and required longer etching times to become hydrophobic. Cl-Ge(111) samples were produced by etching in 6.0 M HCl(aq) for 20–25 min until hydrophobic. Br-Ge(111) samples were produced by etching in 6.0 M HBr(aq) for 1–3 min.

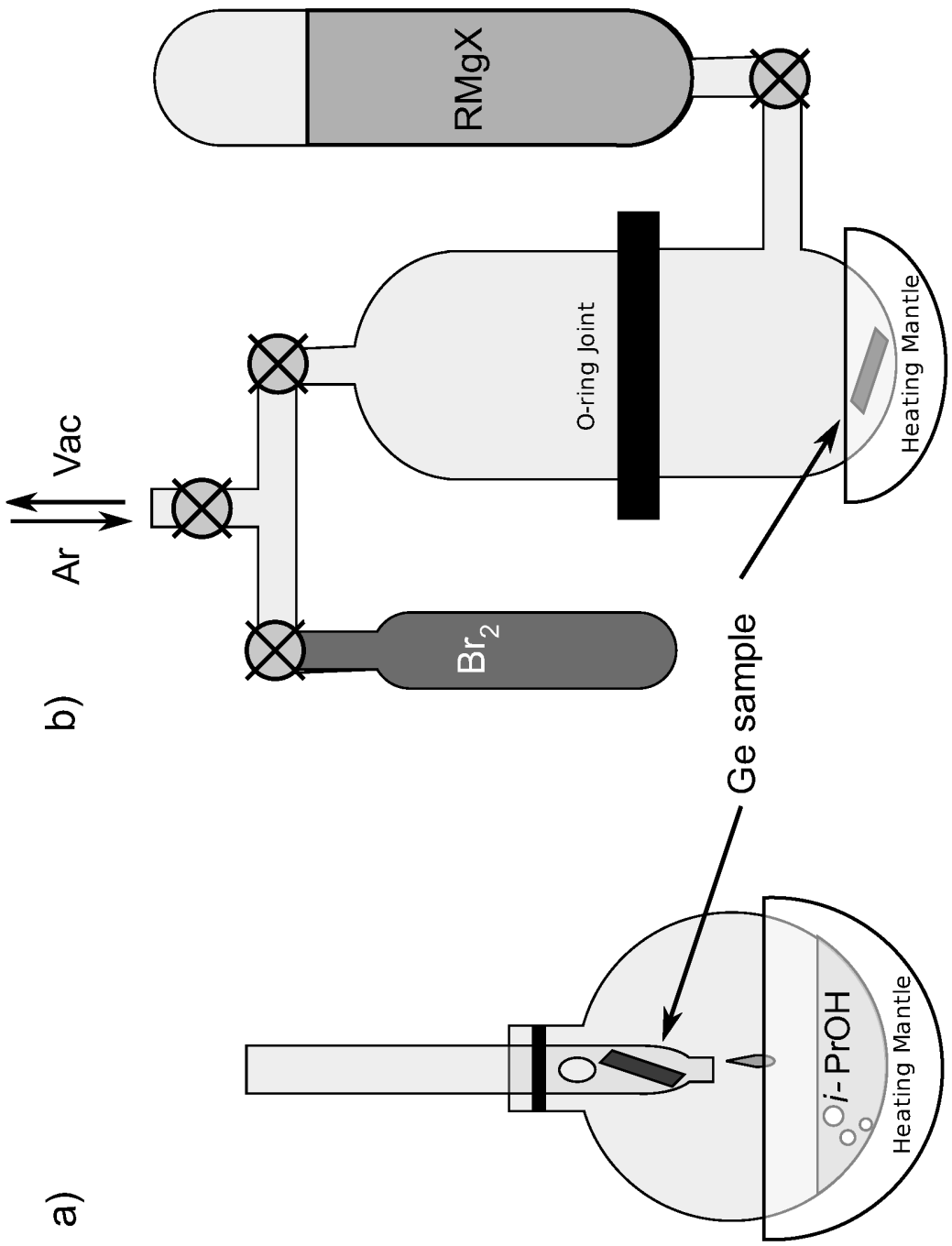

Figure 2.3: Glassware: a. Extractor b. Modified drying chamber

Table 2.1: Procedures of Etching Ge(111)

Etchant Name	step	Composition	duration
HF-6	1	6.0 M HF	20-25 min
HF-12	1	12.0 M HF	8-15 min
HCl-6	1	6.0 M HCl	20-25 min
HCl-9	1	9.0 M HCl	8-10 min
HBr-6	1	6.0 M HBr	1-3 s
HF-NH_4Cl-6	1	6.0 M HF & 6.0 M NH_4Cl	20 min[a]
Superoxol-6	1	1.6 M H_2O_2 & 5.1 M HF	1-3 s
	2	6.0 M HF	3-6 min
Superoxol-6-HCl	1	1.6 M H_2O_2 & 5.1 M HF	1-3 s
	2	6.0 M HCl	>45 min[b]
Superoxol-12	1	1.6 M H_2O_2 & 5.1 M HF	1-3 s
	2	12.0 M HF	30 s

a became coated with hydrocarbons and did not lose hydrophobicity in prolonged contact with water or etchant.
b did not become hydrophobic

Immediately after removal from the etchant, the hydrophobic sample was blown dry with nitrogen and placed in a modified drying chamber, depicted in Figure 2.3b. The chamber was evacuated and backfilled with argon several times. For all but the HBr-etched samples, when the chamber pressure was below 20 mTorr, the vacuum line was closed and the chamber was backfilled with Br_2. After 2–3 minutes, the valve to vacuum was re-opened and the Br_2 captured in a liquid nitrogen trap. Once the pressure was again below 20 mTorr, the low vapor pressure organomagnesium or organolithium solution was added until the sample was completely immersed, and the chamber backfilled with argon. Reactions involving the lithium reagent were not heated, but the organomagnesium solution was heated to 60–70°C and left to react for 3–12 h. In the case of decylmagnesium bromide, the reaction was left for 20–24 h. Once the solution had cooled, the sample was removed and rinsed successively with isopropanol, methanol, water, 1.7 M acetic acid(aq) (to remove magnesium hydroxide), water, methanol, isopropanol, then placed back into the extractor or detergent solution until needed.

2.2.2.2 Hydrogermylation

Samples were etched with 6.0 M HF and placed under vacuum in a drying chamber, as described above. 1-Decene was added to the chamber until the sample was completely immersed, then the chamber backfilled with Ar(g) and heated to reflux for 3 h while under a slight positive argon pressure. Once cooled, the sample was removed and rinsed with hexanes and isopropanol, then placed back into the extractor until further needed.

2.2.2.3 Thiolation

Methanethiol solutions were prepared just prior to use by passing methanethiol vapor through isopropanol. HF etched samples and the thiol solution were placed in a sealed polypropylene container overnight. After removal from the solution, the sample was rinsed with isopropanol and methanol.

2.2.3 Elemental Surface Chemical Analysis

2.2.3.1 Instrumentation

Measurements were performed at vacuum pressures of $10^{-10}-10^{-8}$ Torr with an M-probe spectrometer interfaced with a computer running ESCA200 Capture software (Service Physics). The monochromatic X-ray line was 1486.6 eV Al Kα directed at 35° to the sample surface. Photoelectrons were collected with a hemispherical analyzer mounted at a 35° angle to the sample surface. The samples were conductive so correction for sample charging was not necessary.

Survey spectra were collected with low resolution settings. Higher resolution scans were collected at settings yielding a full-width at half-maximum of ∼0.76 eV.

2.2.3.2 Analysis

Peak fitting of the detailed scans was performed with ESCA2000 Analysis software (Service Physics). Individual peaks of the Ge 3d and Br 3d doublets were set to have identical asymmetry and Gaussian shape, and a $\frac{5}{2} : \frac{3}{2}$ height ratio of 0.69. All other parameters were allowed to float. Sensitivity factors used for this instrument Br, Ge,

Si, and C were 3.16, 1.62, 0.9, and 1.0, respectively.

Atomic diameters were estimated from the inverse cube root of the atomic density,

$$a = \sqrt[3]{A.W./\rho N_A} \tag{2.11}$$

with $A.W.$ being the atomic weight, ρ the density, and $N_A$is Avogadro's number. The sensitivity factors were obtained from the software. Parameters used to calculate the overlayer thicknesses and equivalent monolayer coverages are collected in Table 2.2.

Table 2.2: XPS Analysis Parameters

element	XPS line	SF(a.u.)	λ(nm)	a(nm)	other		
Ge	3d (30 B. eV)	1.62	3.51	0.283	θ	35	degrees
Br	3d (70 B. eV)	3.16	3.46	0.350	$I^0_{Ge}/I^0_{GeO_x}$	1.51	
C	1s (285 B. eV)	1	3.19	0.369	$\lambda_{Ge,bulk}$	2.36	nm
Si	2p (100 B. eV)	0.9	3.42	0.272			

Table 2.3: Hydrocarbon Coverages

Sample Type	d_{ov} [a] (nm)	d_{ox} (nm)	Φ_{ov} [b] (ML)	% oxidized
CH_3-Ge(111)	1.2 ± 0.2	-	1.6 ± 0.2	-
CH_3-Si(111)	1.3 ± 0.2	-	1.7 ± 0.2	-
1-Decene + H-Ge	2.6 ± 0.2	0.20 ± 0.03	-	30 ± 10
$C_{10}H_{21}MgBr$ + Br-Ge	2.2 ± 0.2	0.06 ± 0.06	-	10 ± 10

a. calculated using total C 1*s* signal

b. calculated using 284 B. eV component only

2.3 Results

Table 2.3 summarizes the calculated overlayer coverages.

2.3.1 Inorganic Modification

Although H atoms are not visible in XPS, it can be seen in Figures 2.4 and 2.5 that etching with 9.0 M HF(aq) is effective in removing the oxide. With one hour in lab air, there is significant oxidation. From the integrated area under the low, broad peak in Figure 2.6, the oxide was calculated to be 0.7 ML.

Figure 2.4: Ge 3d region of HF-etched Ge(111)

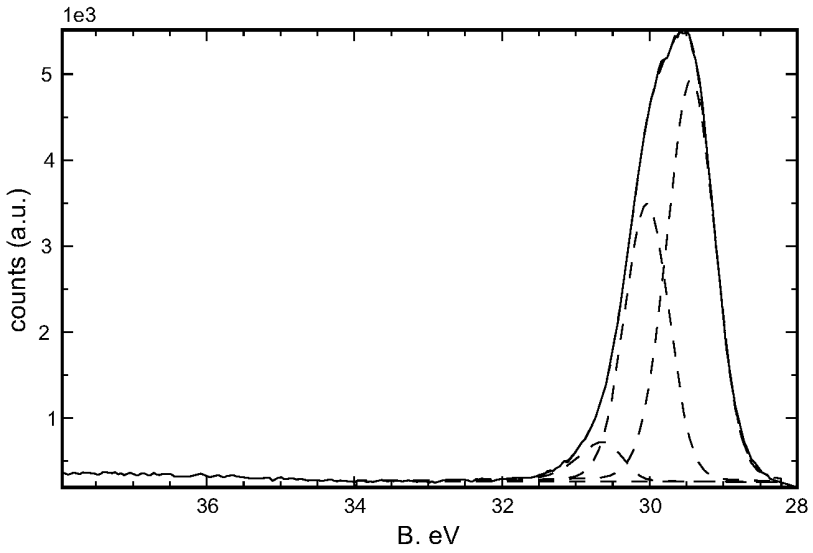

Figure 2.5: Ge 2p region of HF-etched Ge(111)

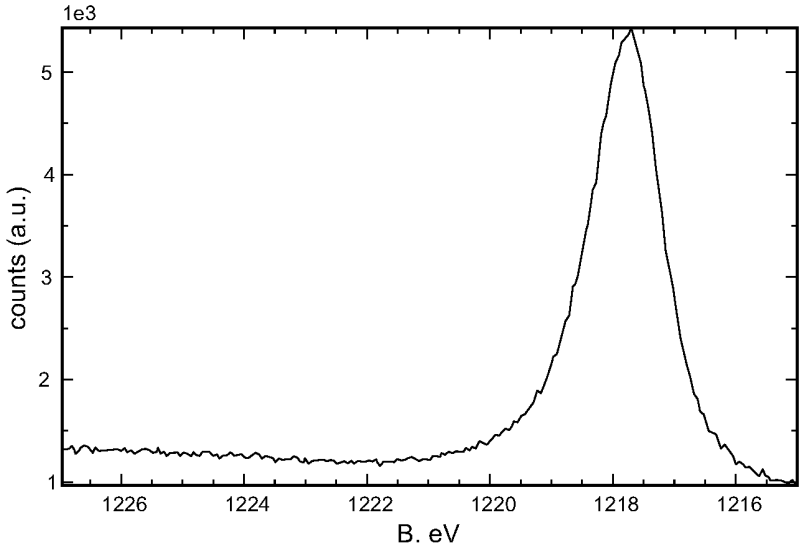

Figure 2.6: Ge 3d region of HF-etched Ge(111) after one hour exposure to air

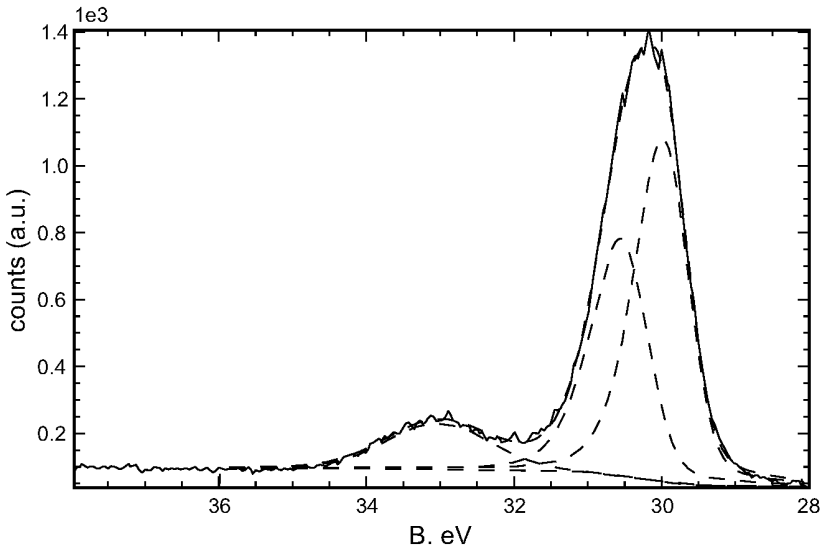

Figure 2.7: Ge 2p region of HF-etched Ge(111) after one hour exposure to air

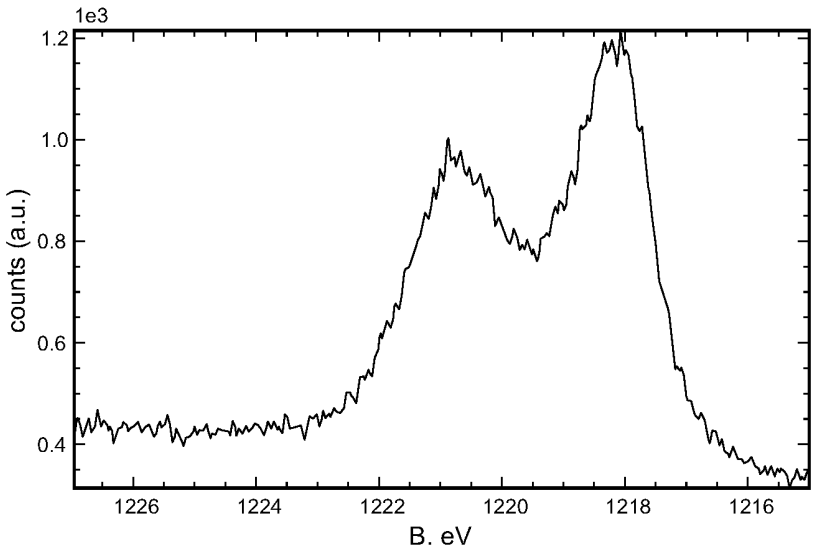

The lack of a significant O 1s peak in the survey spectrum Figure 2.8 on page 34, and the lack of noticeable higher B. eV components in the Ge 3d or Ge 2p spectra, Figures 2.9 and 2.10, show that hydrogen-terminated surfaces immediately treated with Br_2 vapor show little sign of oxidation. From the Br 3d peak intensity, shown in Figure 2.11, initial surface coverages are calculated to be 1.0 $\pm$ 0.1 ML. Halogenated surfaces show much slower rates of oxidation compared to H-Ge(111), but are not air-stable over the long term. After four days exposure to lab air, there is an appearance of 0.3 ML oxide, and a reduction of the Br 3d signal to 0.5 ML. Surfaces that had been etched with 6.0 M HCl(aq) prior to Br_2 exposure displayed 0.5 ML Br, as determined from the ratio of the areas of the Br 3d and Ge 3d peaks, seen in Figures 2.15 and 2.13. The Ge 2p and Ge 3d, shown in Figures 2.14 and 2.13, do not display noticeable high B. eV components indicative of oxidized surface species. Evidence for Cl components can be seen from the small peak at 270 B. eV in the survey spectrum of Figure 2.12, but the Cl peaks were not clear in detailed scans and the coverage was not calculated.

Figure 2.8: Survey of Br-Ge(111) from HF-etched precursor

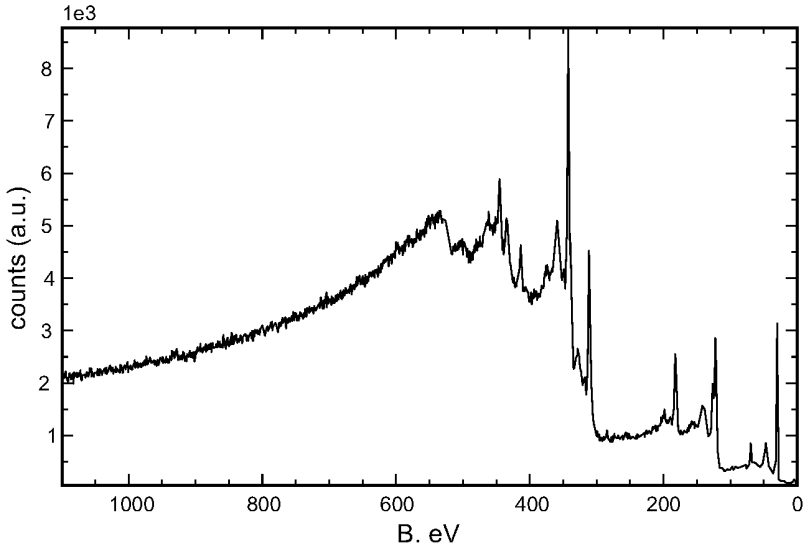

Figure 2.9: Ge 3d region of Br-Ge(111) from HF-etched precursor

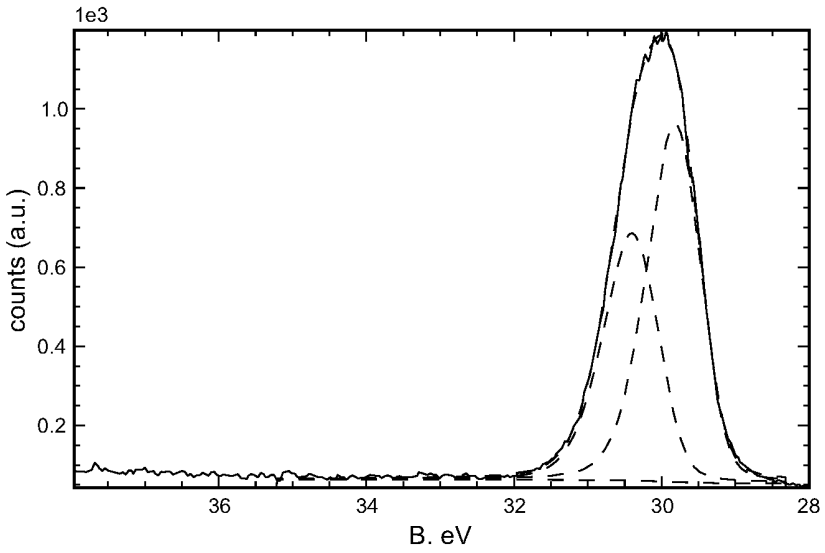

Figure 2.10: Ge 2p region of Br-Ge(111) from HF-etched precursor

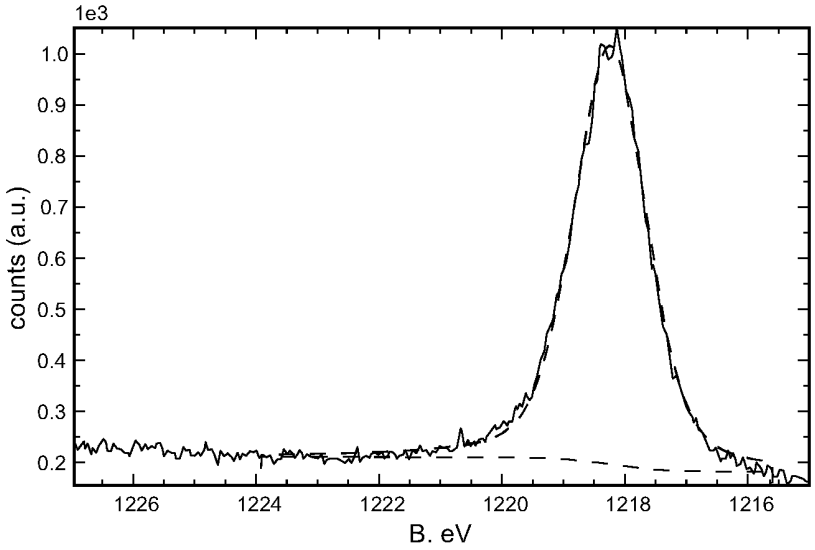

Figure 2.11: Br 3d region of Br-Ge(111) from HF-etched precursor

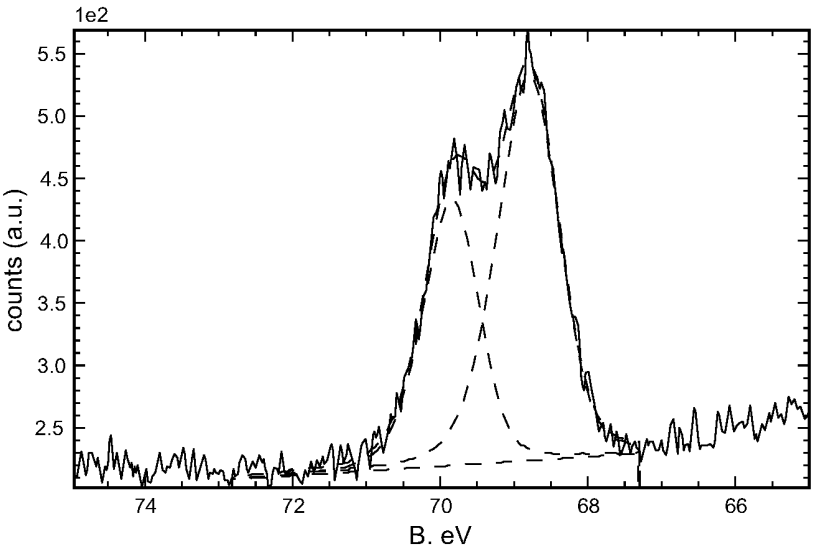

Figure 2.12: Survey of Br-Ge(111) from HCl-etched precursor

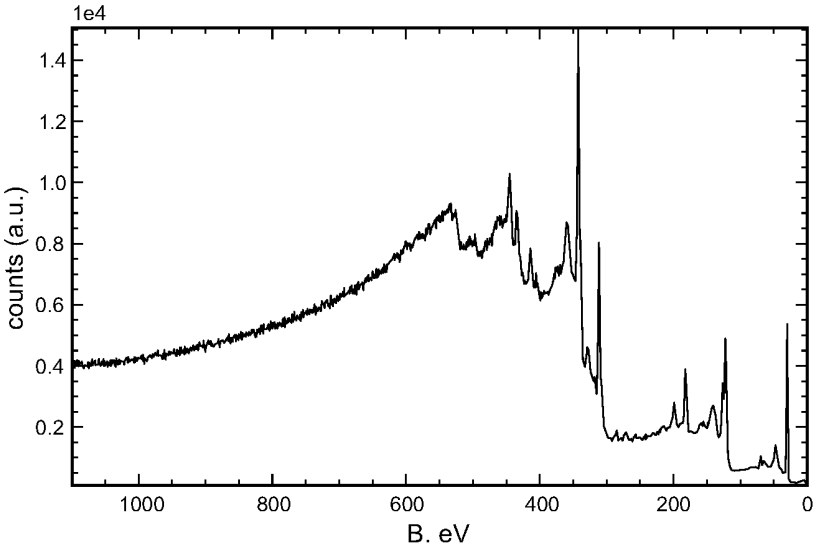

Figure 2.13: Ge 3d of Br-Ge(111) from HCl-etched precursor

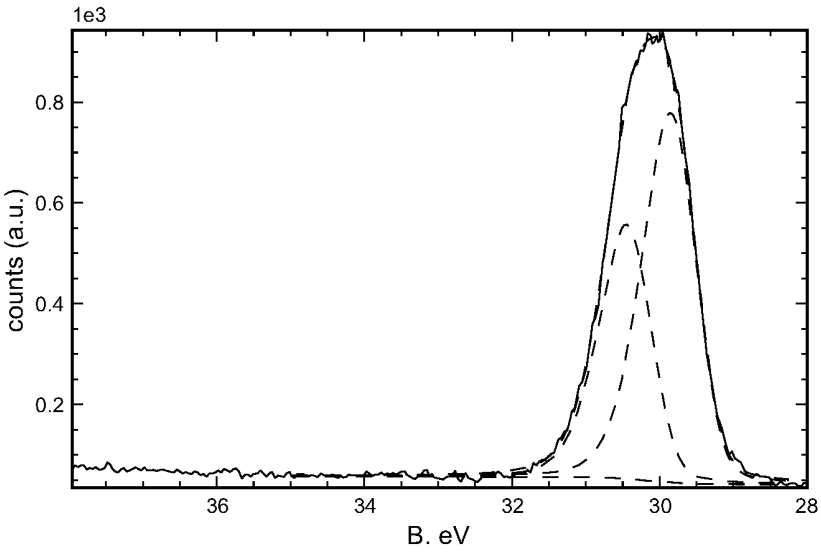

Figure 2.14: Ge 2p of Br-Ge(111) from HCl-etched precursor

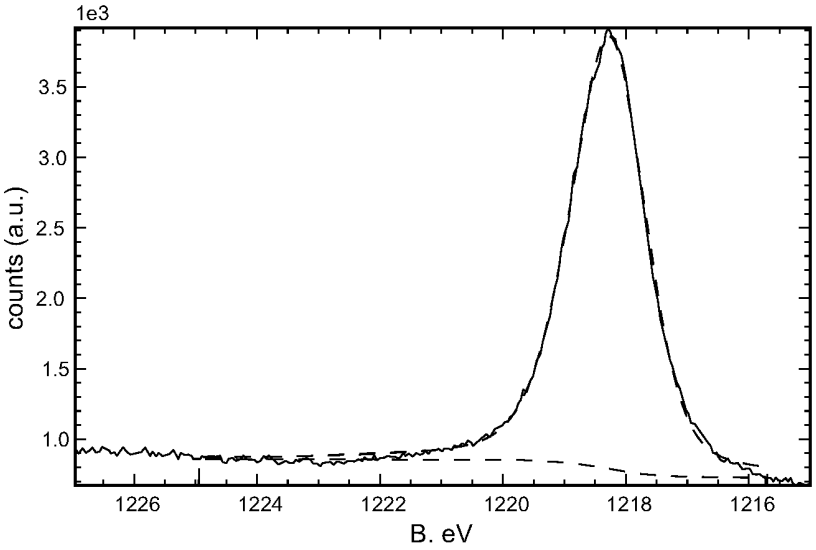

Figure 2.15: Br 3d region of Br-Ge(111) from HCl-etched precursor

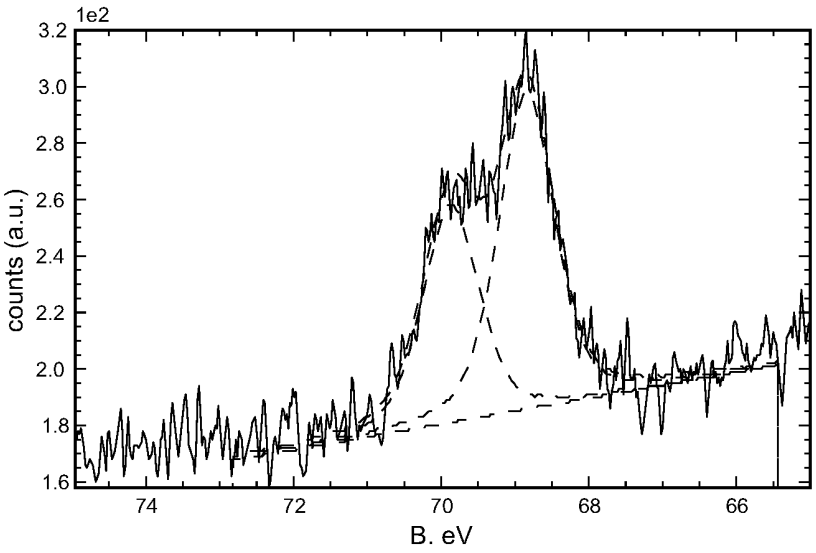

Methanethiol modified surfaces were initially hydrophobic and displayed no detectable oxide. The sensitivity factor of the S $2p$ peak was high enough for the sulfur layer to be detectable, but as can be seen in Figure 2.2 on page 17 the 160 B. eV region does not have a clear background, and obtaining an accurate intensity value for monolayer calculation was not possible. After one day, significant oxidation could be seen in the Ge $3d$ peak displayed shown in Figure 2.19, calculated to be 0.3–0.5 ML, and the S$2p$ peak was no longer detectable, as seen in Figure 2.20.

Figure 2.16: Survey of CH_3S-Ge(111)

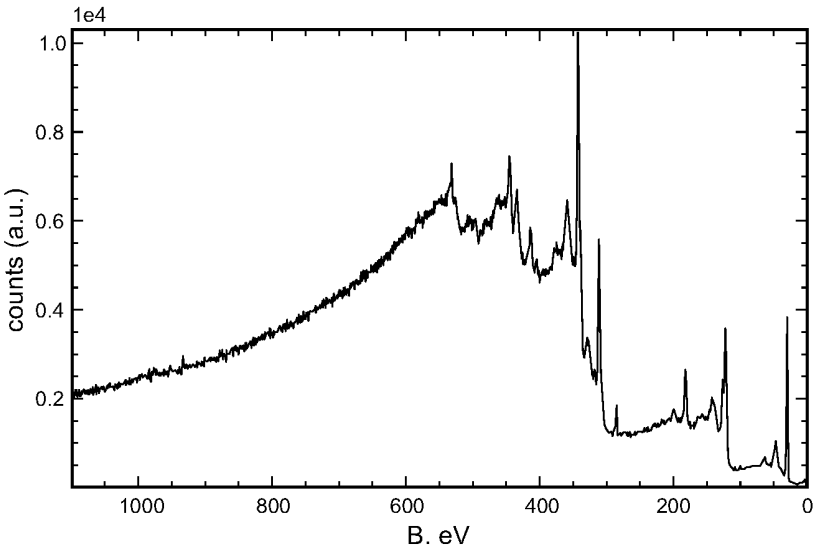

Figure 2.17: S 2p region of CH_3S-Ge(111)

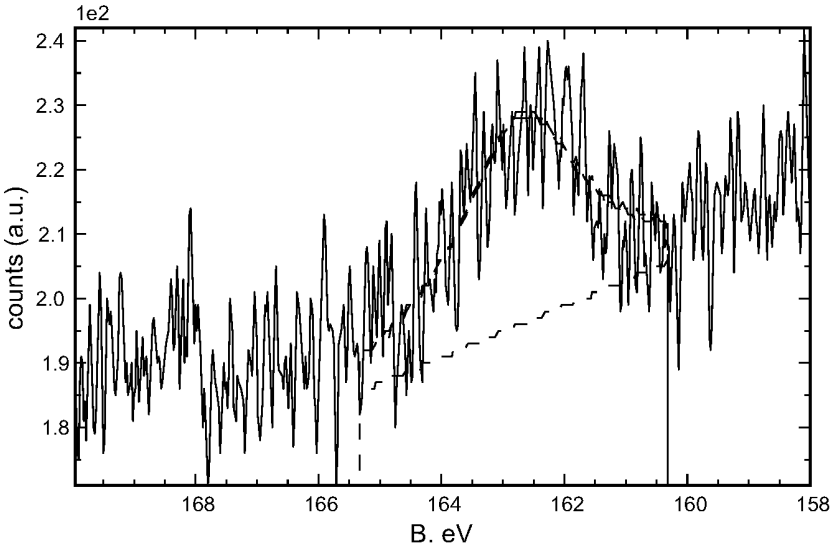

Figure 2.18: Ge 3d region of CH_3S-Ge(111)

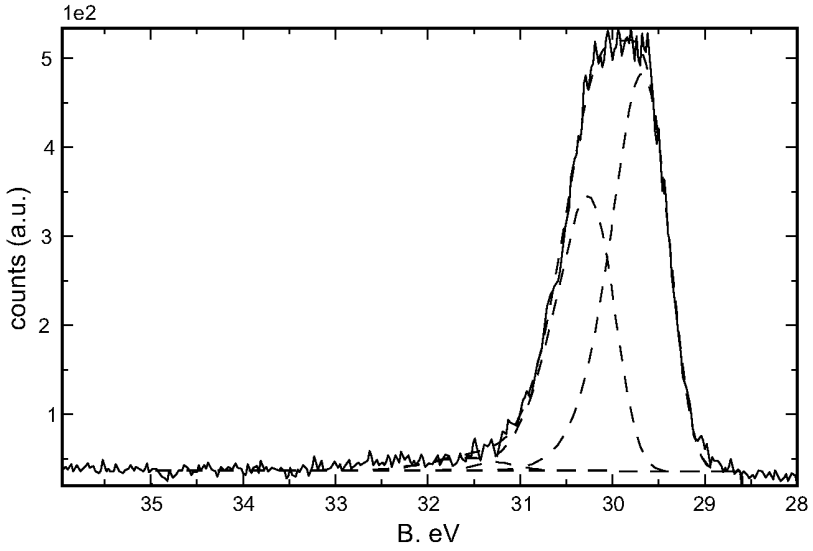

Figure 2.19: Ge 3d region of CH_3S-Ge(111) after 24 hours in air

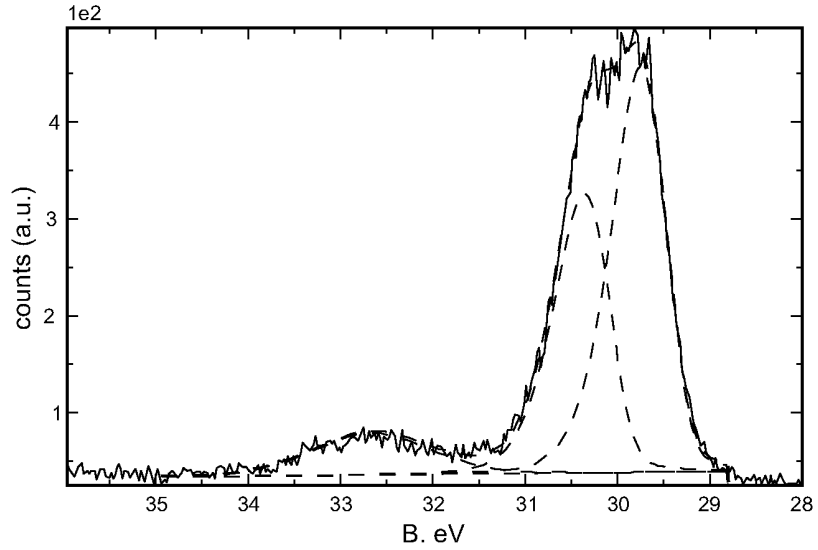

Figure 2.20: S 2p region of CH_3S-Ge(111) after 24 hours in air

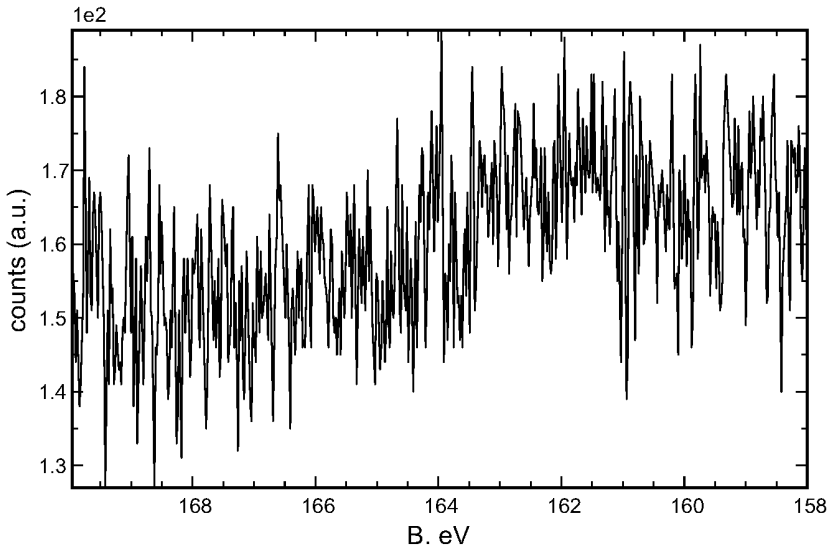

2.3.2 Alkylation

2.3.2.1 Methyl-Terminated Surfaces

Methyl-terminated surfaces showed little sign of oxidation, as seen in Figures 2.21, 2.23, and 2.22, even after the sample had been held in an isopropanol reflux or sonication in detergent solutions for several hours. Such surfaces were stable for at least one week. The lower B eV peak seen in Figure 2.24 is from the surface-capping methyl group. The ratio of the integrated area of the 284.3 B eV peak, I_C, to the integrated area of the Ge 3d peak, I_{bulk}, normalized for element sensitivity, was 0.15 ± 0.02. This is virtually identical to what is observed for CH_3-Si(111) surfaces. Measured by AFM, the surface roughness was 8–13 Å. The value of $I_C : I_{bulk}$ had no strong dependence upon initial etching method.

Figure 2.21: Survey of CH_3-Ge(111)

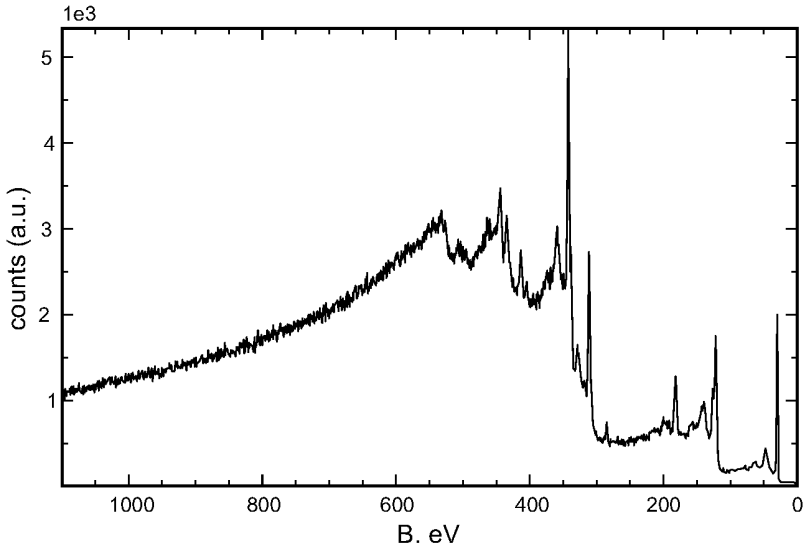

Figure 2.22: Ge 3d region of CH_3-Ge(111)

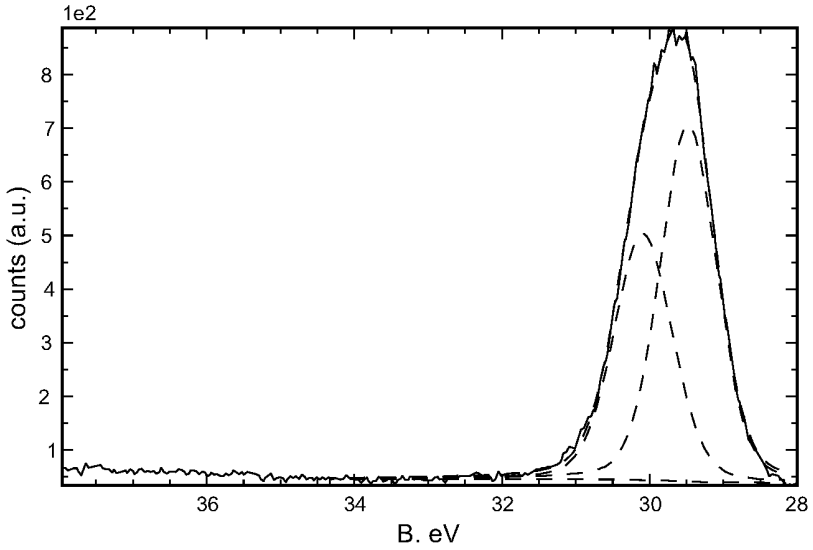

Figure 2.23: Ge 2p region of CH_3-Ge(111)

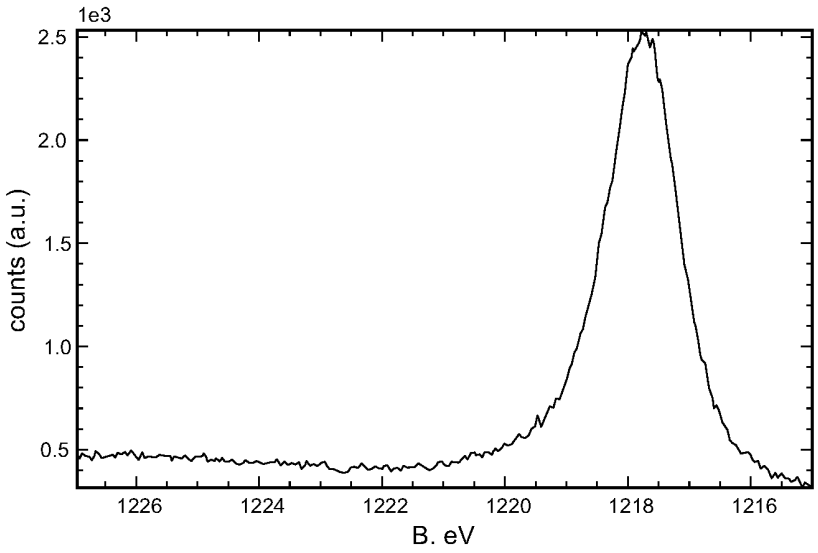

Figure 2.24: C 1s region of CH_3-Ge(111)

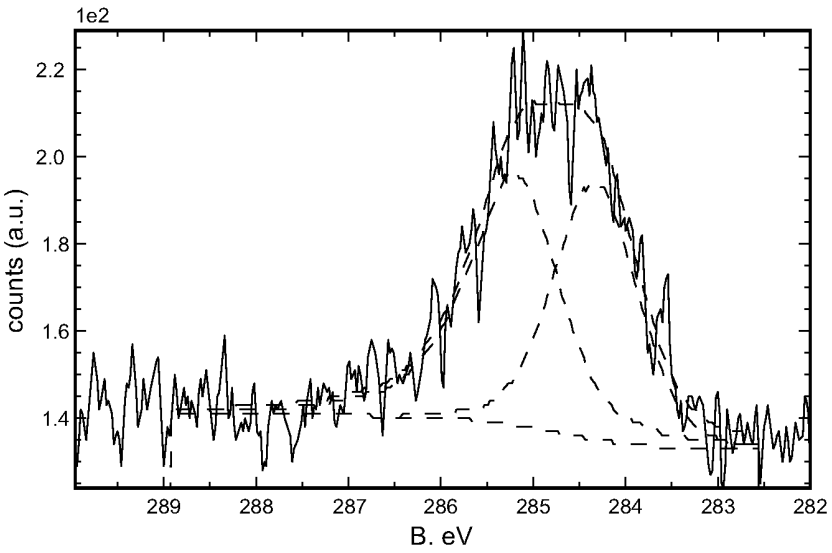

2.3.2.2 Decyl-Terminated Surfaces

Surfaces decyl-terminated through thermal hydrogermylation often showed signs of oxidation of 20–40% of the surface, evident in the higher B eV peaks in Figures 2.28 and 2.29, while similar surfaces prepared through the Grignard alkylation had oxidation levels at or below the 10% detection limit, as evidenced by the lack of a higher B eV component in Figure 2.26 . The long hydrocarbon chain of the decyl groups, in addition to any adventitious hydrocarbon, obscured the C-Ge peak at 284.3 B eV with a large 285 B eV component, as seen in Figure 2.27, so no reliable estimate of the fractional monolayer coverage was possible. The hydrocarbon overlayer thicknesses resulting from both methods were similar, 2.2 ±0.2 nm for the Grignard route, 2.1 ± 0.2 nm for the hydrogermylation.

Figure 2.25: Survey of $C_{10}H_{21}$-Ge(111) prepared from Grignard reagent

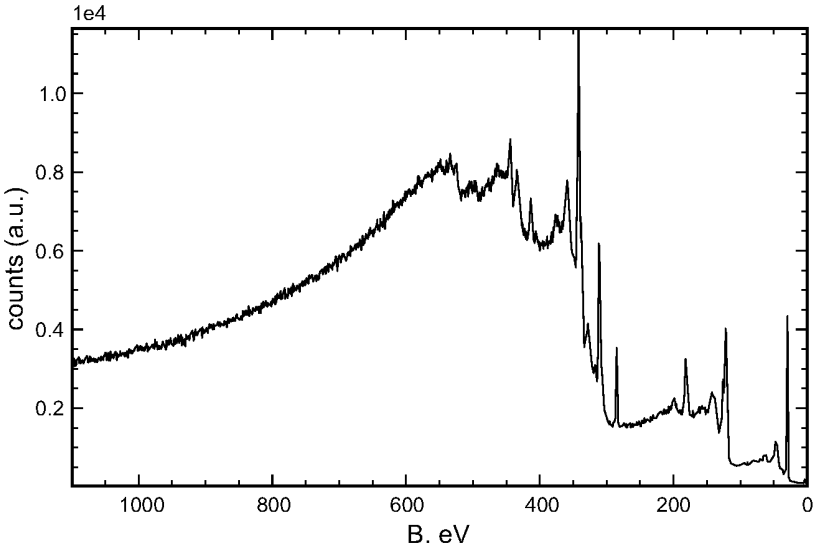

Figure 2.26: Ge 3d region of $C_{10}H_{21}$-Ge(111) prepared from Grignard reagent

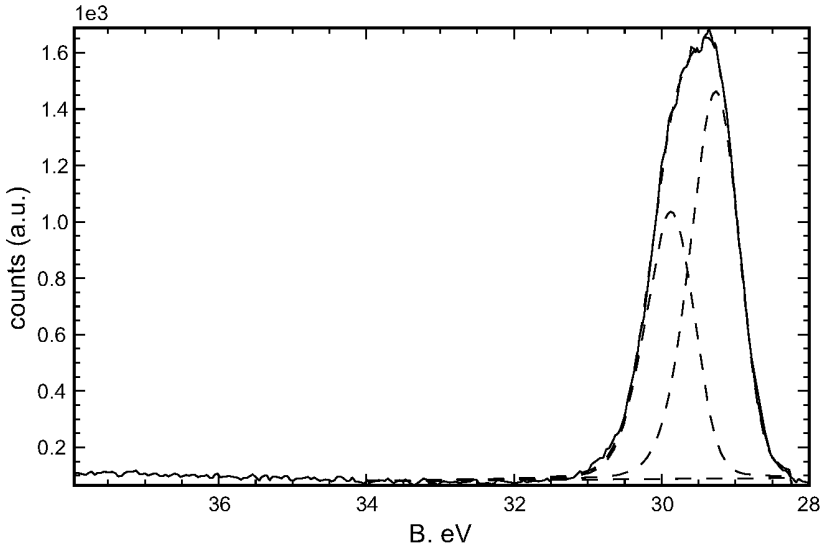

Figure 2.27: C 1s region of $C_{10}H_{21}$-Ge(111) prepared from Grignard reagent

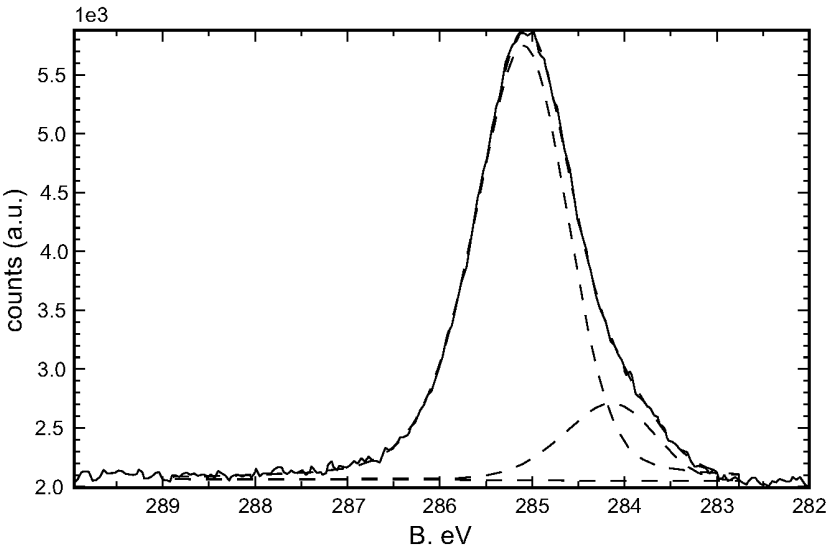

Figure 2.28: Ge 2p region of $C_{10}H_{21}$-Ge(111) prepared from 1-decene

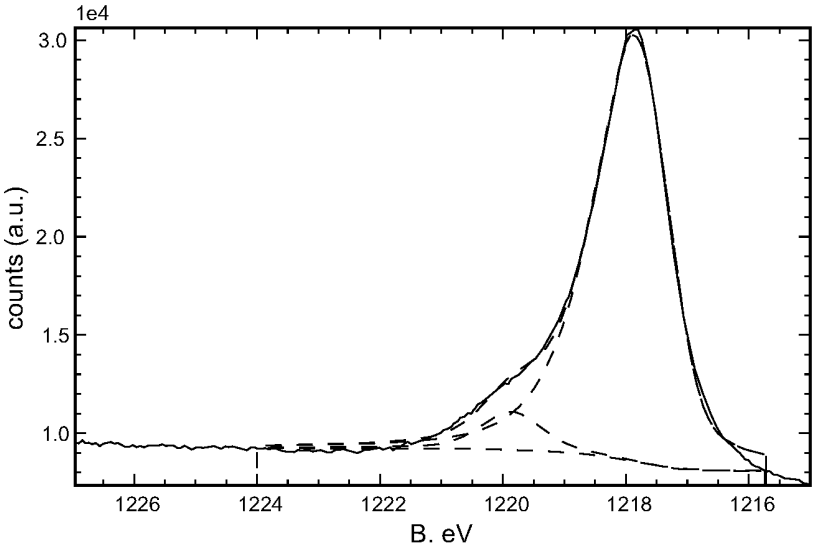

Figure 2.29: Ge 3d region of $C_{10}H_{21}$-Ge(111) prepared from 1-decene

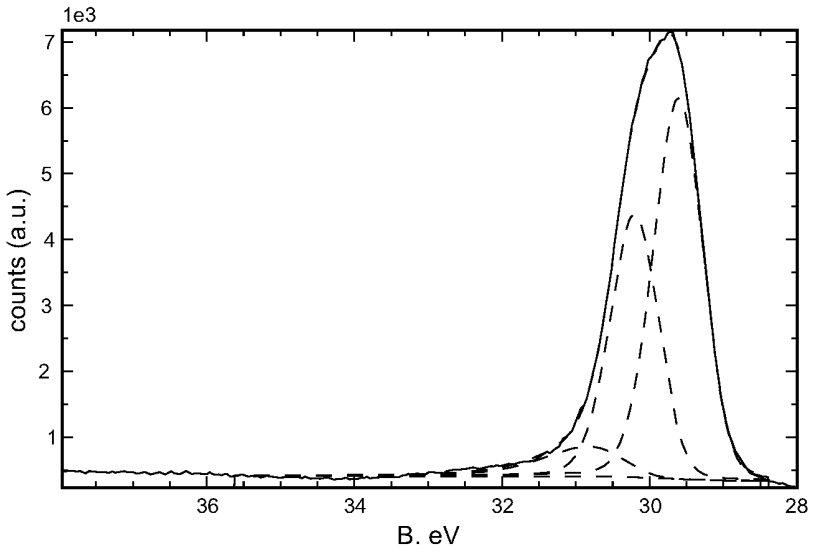

2.4 Discussion

2.4.1 Inorganic Surface Groups

Hydrogen-terminated and halogen-terminated Ge surfaces do not provide chemically stable surfaces, but are useful as intermediates for further processing. The higher reactivity of the H-Ge(111) surface relative to the halogen-terminated surfaces is not simply explained by the bond dissociation energies, for the H-Ge bond is intermediate, at 290 kJ/mol, between Cl-Ge (356 kJ/mol) and Br-Ge (276 kJ/-mol).[31] The chloride-terminated surfaces are believed to be well ordered, but the HF-etched surfaces are not, which would be expected to cause differences in reactivity.[15,16] This atomic roughness could also explain the discrepancy between earlier reports of H-Ge(111) stability and what has been observed more recently, including the work described here.[13,26]

Thiol termination of Ge continues to receive attention because the procedure is simple, the concept is reminiscent of Au-thiol monolayer system, and H-, Cl-, and Br-terminated surfaces are not stable.[6,26] Monolayers attached via a Ge-S bond are not as stable as those attached by a Ge-C bond, but that does not rule out their use as a stable intermediate.[32] In this study, the Ge-S bond was of interest so methanethiol was used, despite the inconvenience of handling, so that the surface was not protected simply by being buried under a thick hydrocarbon layer. The procedure was not optimized, so the presence of oxygen on the surface could have been further minimized. If the Ge-S-C bonding was not stable, the small thiol molecule could be expected to easily desorb. This is confirmed in Figure 2.20 on page 40 by the disappearance of

the S 2p after one day exposure to air.

2.4.2 Alkyl Groups

2.4.2.1 Methyl

As has been established for CH_3-Si(111), methylation of the Ge(111) surface protects the surface from chemical oxidation by atmospheric conditions. After normalization for differing sensitivity factors, the ratio of surface-bound C 1s XPS line to the bulk Ge 3d line, $I_{C1s} : I_{Ge3d}$, is nearly identical to the $I_{C1s} : I_{Si2p}$ ratio measured in the CH_3-Si(111) surfaces prepared in this work and in measurements previously reported by others.[33] From this, it can be concluded that there is complete or near complete termination of atop Ge bond sites, and the final surface is comparable to that of Si. The 12±2 Å overlayer thickness (see Table 2.3) is too large for a methyl group with a van der Waals radius of 2.2 Å.[27] However, if the adventitious hydrocarbon peak, which can be seen to comprise just over half the entire C 1s signal, is discounted, a measured value of 6 ±2 Å thickness is obtained. Such a value is justifiable if the surface is not atomically smooth over the area of the incident X-ray spot.

A proposed mechanism for the alkylation of the halogenated (or hydrogen-terminated) surface is that alkyl halide impurities are reduced by the Grignard and form radicals, both in solution and on the crystal surface.[34] Evidence of radicals in lithium-halide exchange reactions indicates that the same process is possible for alkyllithium reagents.[35] The report that alkyllithium reagents were ineffective in this type of alkylation raises the question of whether the alkylation mechanism is different for Si and

Ge.[36] In this work however, there were no detectable differences in methylated surfaces prepared from CH_3MgX (X = Cl,Br,I,CH_3) or CH_3Li. This would be consistent with the radical model, which implicates halogenated hydrocarbons as a radical source, because the methyllithium solution was reported by the supplier to contain lithium iodide, and removal of $MgBr_2$ with dioxane, to prepare $(CH_3)_2Mg$ solutions, would have little effect upon halogenated hydrocarbon impurities.

2.4.2.2 Decyl

The long reaction times reported to be necessary for the Grignard alkylation make the quicker one-step hydrogermylation reaction an attractive method of surface passivation. Hydrophobic surfaces with largely non-oxidized surface Ge atoms do indicate that there was surface modification, however it was not as successful as the Grignard reaction route. Both the Grignard alkylation and hydrogermylation routes yielded layer thicknesses that were higher than expected, but if the adventitious hydrocarbon contribution to the C 1*s* signal is assumed to be the same for both the $C_{10}H_{21}$-Ge(111) and CH_3-Ge(111) surfaces and may be similarly subtracted, the resulting 15–16 Å thickness is in better agreement with that seen on Si(111).[37]

The majority of reports on successful hydrogermylation characterize the surfaces by IR, XPS, and contact angle.[24,25,38,39] Of the reports that address the issue, the authors concede that there is some oxidation.[25,38] Considering the higher temperatures necessary in hydrogermylation compared to Grignard alkylation, it is not surprising that there would be degradation of the H-Ge(111). Because the alkyllithium and alkylmagnesium reagents react with water, the reaction conditions for the two-

step alkylation are dry, even if there are other oxygen-containing species present. It should be noted that there can be significant variability in the quality of Si(111) surfaces modified by reaction with alkenes, so the occurrence of oxide growth may be eliminated with further optimization of the reaction conditions.[40,41]

2.5 Conclusion

Alkyl monolayers prepared through a milder version of the surface modification technique first attempted almost 50 years ago show initial low oxygen content and long-term resistance to atmospheric oxidation. XPS measurements confirm that the hydrogen-terminated surface is unstable and that the brominated surfaces are slower to oxidize but do not demonstrate long-term stability. The low level of oxidation present in the final alkylated surfaces demonstrates that despite this instability, the hydrogen- and bromine-terminated surfaces are suitable intermediates for the production of stable alkylated surfaces. Methylmagnesium halide, dimethylmagnesium, and methyllithium proved to be effective methylating reagents.

Two other surface passivation techniques were attempted but were not as successful. While it may be possible to prepare low oxygen content monolayers through the use of alkanethiols, the Ge-S bond does not show long term stability. Hydrogermylation does provide a one-step route to a stable overlayer grafted with a stable Ge-C bond, but the initial oxide content was higher than what is seen in the Grignard alkylation method. Furthermore, both thiolation and hydrogermylation reactions are better suited to production of monolayers of larger alkane groups, while the Grignard

alkylation method is applicable to methyl groups and larger alkanes.

Bibliography

[1] Cullen, G.; Amick, J.; Gerlich, D. *J. Electrochem. Soc.* **1962**, *109*, 124–127.

[2] Bansal, A.; Li, X.; Lauermann, I.; Lewis, N.; Yi, S.; Weinberg, W. *J. Am. Chem. Soc.* **1996**, *118*, 7225–7226.

[3] Bansal, A.; Lewis, N. *J. Phys. Chem. B* **1998**, *102*, 4058–4060.

[4] Bolts, J. M.; Wrighton, M. S. *J. Am. Chem. Soc.* **1978**, *100*, 5257–5262.

[5] Brunco, D. et al. *J. Electrochem. Soc.* **2008**, *155*, H552–H561.

[6] Ardalan, P.; Musgrave, C.; Bent, S. *Langmuir* **2009**, *25*, 2013–2025.

[7] Kamata, Y.; Ino, T.; Koyama, M.; Nishiyama, A. *Applied Physics Letters* **2008**, *92*, 063512.

[8] Rivillion, S.; Chabal, Y. J.; Amy, F.; Kahn, A. *Appl. Phys. Lett.* **2005**, *87*, 253101.

[9] Maroun, F.; Ozanam, F.; Chazalviel, J.-N. *J. Phys. Chem. B* **1999**, *103*, 5280–5288.

[10] Kosuri, M.; Cone, Q., R. Li; S.M., H.; Bunker, B.; Mayer, T. *Langmuir* **2004**, *20*, 835–840.

[11] Higashi, G.; Chabal, Y.; Trucks, G.; Raghavachari, K. *Appl. Phys. Lett.* **1990**, *56*, 656–658.

[12] Bodlaki, D.; Yamamoto, D.; Waldeck, D.; Borguet, E. *Surf. Sci.* **2003**, *543*, 63–74.

[13] Deegan, T.; Hughes, G. *Appl. Surf. Sci.* **1998**, *123/124*, 66–70.

[14] Fouchier, M.; McEllistrem, M.; Boland, J. *Surf. Sci.* **1997**, *385*, L905–L910.

[15] Lu, Z. *Appl. Phys. Lett.* **1996**, *68*, 1996.

[16] Cao, S.; Tang, J.-C.; Shen, S. *J. Phys.: Condens. Matter.* **2003**, *15*, 5261–5268.

[17] Sun, S.; Sun, Y.; Lee, D.-I.; Pianetta, P. *Appl. Phys. Lett.* **2006**, *89*, 231925.

[18] Wang, D.; Dai, H. *Appl. Phys. A* **2006**, *85*, 217–225.

[19] Newstead, K.; Robinson, A.; Patchett, A.; Prince, N.; McGrath, R.; Whittle, R.; Dudzik, E.; McGovern, J. T. *J. Physics: Cond. Matt.* **1992**, *4*, 8441–8446.

[20] Anderson, G.; Hanf, M.; Norton, P.; Lu, Z.; Graham, M. *Appl. Phys. Lett.* **1995**, *66*, 1123–1125.

[21] Lyman, P.; Sakata, O.; Marasco, D.; Breneman, K.; Keane, D.; Bedzyk, M. *Surf. Sci.* **2000**, *462*, L594–L598.

[22] Frank, M. M.; Koester, S. J.; Copel, M.; Ott, J. A.; Paruchuri, V. K.; Shang, H.; Loesing, R. *Appl. Phys. Lett.* **2006**, *89*, 112905.

[23] Han, S. M.; Ashurst, W. R.; Carraro, C.; Maboudian, R. *J. Am. Chem. Soc.* **2001**, *123*, 2422–2425.

[24] Sharp, I.; Schoell, S.; Hoeb, M.; Brandt, M.; Stutzmann, M. *Appl. Phys. Lett.* **2008**, *92*, 223306.

[25] Choi, K.; Buriak, J. *Langmuir* **2000**, *16*, 7737–7741.

[26] Ardalan, P.; Sun, Y.; Pianetta, P.; Musgrave, C. B.; Bent, S. F. *Langmuir* **2010**, *26*, 8419–8429.

[27] Rivillion, S.; Chabal, Y. *J. Phys. IV* **2006**, *132*, 195–198.

[28] Yu, H.; Webb, L.; Heath, J.; Lewis, N. *Appl. Phys. Lett.* **2006**, *88*, 252111.

[29] Pomykal, K. E.; M., F. A.; Lewis, N. *J. Phys. Chem.* **1995**, *99*, 8302–8310.

[30] Haber, J. A.; Lewis, N. S. *J. Phys. Chem. B* **2002**, *106*, 3639–3656.

[31] *CRC Handbook of Chemistry and Physics*; Lide, D. R., Ed.; CRC Press LLC: Boca Raton, 1999.

[32] S.M., H.; Ashurst, W.; Carraro, C.; Maboudian, R. *J. Am. Chem. Soc.* **2001**, *123*, 2422–2425.

[33] Nemanick, E.; Hurley, P.; Brunschwig, B.; Lewis, N. *J. Phys. Chem. B* **2006**, *110*, 14800–14808.

[34] Fellah, S.; Boukherroub, R.; Ozanam, F.; Chazalviel, J.-N. *Langmuir* **2004**, *20*, 6359–6364.

[35] Seyferth, D. *Organometallics* **2006**, *25*, 2–24.

[36] He, J.; Lu, Z.; Mitchell, S.; Wayner, D. *J. Am. Chem. Soc.* **1998**, *120*, 2660–2661.

[37] Linford, M.; Fenter, P.; Eisenberger, P.; Chidsey, C. *J. Am. Chem. Soc.* **1995**, *117*, 3145–3155.

[38] Hanrath, T.; Korgel, B. *J. Am. Chem. Soc.* **2004**, *126*, 15466–15472.

[39] Chen, R.; Bent, S. *Chem. Mater.* **2006**, *18*, 3733.

[40] Webb, L.; Lewis, N. *J. Phys. Chem. B* **2003**, *107*, 5404–5412.

[41] Aureau, D.; Rappich, J.; Moraillon, A.; Allongue, P.; Ozanam, F.; Chazalviel, J.-N. *J. Electroanal. Chem.* **2010**, *646*, 33–42.